Optical Properties and Thermal Stability of Pulsed Sputter Deposited $Cr_xO_y/Cr/Cr_2O_3$ Solar Selective Coatings

N. Selvakumar*, H.C. Barshilia, K.S. Rajam
Surface Engineering Division,
National Aerospace Laboratories (CSIR),
Bangalore–560 017, India
E-mail: selvakumar@nal.res.in

A. Biswas
Spectroscopy Division,
Bhabha Atomic Research Center,
Mumbai–400 085, India

Abstract

Spectrally selective $Cr_xO_y/Cr/Cr_2O_3$ multilayer absorber coatings were deposited on copper (Cu) substrates using a pulsed sputtering system. The Cr targets were sputtered using asymmetric bipolar-pulsed DC generators in $Ar+O_2$ and Ar plasmas to deposit a Cr_xO_y (bottom layer)/Cr/Cr_2O_3 (top layer) coating. High absorptance (0.899-0.912) and low emittance (0.05-0.06) were achieved by optimizing the composition and thicknesses of the individual layers. In order to study the thermal stability of the $Cr_xO_y/Cr/Cr_2O_3$ coatings, they were subjected to heat treatment (in air and vacuum) at different temperatures and durations. The coating deposited on Cu substrates exhibited high solar selectivity (α/ε) of 0.895/0.06 even after heat-treatment in air up to 300 °C for 2 h. In the case of vacuum annealing, for temperatures greater than 500 °C the outward diffusion of Cu was the dominating degradation mechanism. Studies on the accelerated aging tests indicated that the absorber coatings on Cu were stable in air up to 250 h at 250 °C with a solar selectivity of 0.898/0.11.

Surface Modification Technologies XXIII
Edited by T. S. Sudarshan, U. Kamachi Mudali and Baldev Raj

1.0. Introduction

Efficient photo-thermal conversion of solar energy requires spectrally selective surfaces with high solar absorptance (α) in the wavelength range of 0.3–2.5 μm and low thermal emittance (ε) in the infrared region (IR; λ ≥ 2.5μm) [1]. Spectral selectivity can be achieved using various concepts such as absorber-reflector tandem, cermet coatings and multilayer absorbers [2-6]. In cermet coatings, the metal content gradually decreases from substrate-coating interface to the surface of the absorber. One of the well-known examples of a cermet coating is electrodeposited black chrome (Cr-Cr_2O_3 cermet), which has been widely used for domestic hot water applications [7, 8]. Typically, the black chrome coatings exhibit absorptance of 0.90-0.95 and emittance of 0.1-0.2.

Cr-Cr_2O_3 solar selective coatings are usually prepared using electrodeposition and chemical vapor deposition (CVD) methods [7, 9]. Due to the carcinogenic nature of hexavalent Cr, alternative methods such as sputtering have been used to develop solar selective coatings. There are very few reports in the literature on sputter deposited chromium based absorbers [10, 11]. Both reactive direct current (DC) and radiofrequency (RF) sputtering have been used to deposit Cr_2O_3-Cr absorbers [10-12]. However, insulating oxides cannot be sputtered using DC power supply and RF sputtering suffers from low growth rates and its complexity. With pulsed sputtering it is possible to deposit highly adherent, uniform and dense coatings of dielectric nitride and oxides with high growth rates [13]. In the present investigation, asymmetric bipolar-pulsed DC generators were used to deposit a $Cr_xO_y/Cr/Cr_2O_3$ multilayer absorber coating. Alternate layers of chromium oxide and metallic Cr were deposited by switching on and off the oxygen flow. The thermal stability of these coatings in air and vacuum are discussed in detail. Accelerated aging tests have also been performed on these coatings.

2.0. Experimental Details

$Cr_xO_y/Cr/Cr_2O_3$ coatings were prepared on Cu substrates (dimensions 35 mm × 35 mm × 2 mm) using a reactive DC unbalanced magnetron sputtering system [13]. Before putting the substrates into the vacuum chamber, they were metallographically polished and chemically cleaned. The vacuum chamber was pumped down to a base pressure of 5.0×10^{-4} Pa. High purity Cr (99.95%) targets (diameter = 0.075 m) were used for the deposition of the coatings. Asymmetric bipolar-pulsed generators (frequency = 100 kHz, pulse width = 2976 ns, positive pulse bias = +37 V) were used to sputter the Cr targets [13]. The Cr_xO_y and Cr_2O_3 layers were prepared from the reactive sputtering of Cr targets in Ar + O_2 plasma at a pressure of 1.0×10^{-1} Pa. For the deposition of the bottom Cr_xO_y layer, the power density was 2.5 watts/cm^2 and the oxygen flow rate was 5 sccm. The Cr metal layer was deposited from the non-reactive sputtering of the Cr target in Ar plasma at a pressure of 1.0×10^{-1} Pa. Sputtering was carried out at a power density of 2.5 watts/cm^2 for the Cr metal layer. For the top Cr_2O_3 layer, the power density was 6 watts/cm^2 and the oxygen flow rate was 16 sccm.

The optical properties (α and ε) of the $Cr_xO_y/Cr/Cr_2O_3$ coatings were measured using solar spectrum reflectometer (Model SSR) and emissometer (Model AE) of M/s. Devices and Services. The absorptance and the emittance values were measured at four different positions and the values reported herein are the average of four measurements. The bonding structure of the coatings was characterized by XPS using an ESCA 3000 (V.G. Microtech) system with a monochromatic Al K_α X-ray beam (energy = 1486.5 eV and power = 150 watts).

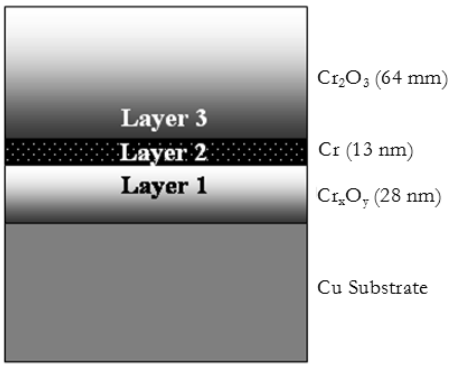

Fig. 1: Schematic diagram of the $Cr_xO_y/Cr/Cr_2O_3$ absorber coating deposited on copper substrate.

Table 1: Optimized process parameters for the deposition of $Cr_xO_y/Cr/Cr_2O_3$ coatings deposited on copper substrates.

Layer	O_2 flow rate (sccm)	Power (Watts)	Substrate Temperature (°C)	Substrate Bias (Volts)	P_o (Pa)	Thickness (nm)
Cr_xO_y	5	100	150	-90	1.0×10^{-1}	28
Cr	-	100	150	-90	1.0×10^{-1}	13
Cr_2O_3	16	300	150	-90	1.0×10^{-1}	64

In order to test the thermal stability, the $Cr_xO_y/Cr/Cr_2O_3$ coatings deposited on Cu substrates were heated in air in a resistive tubular furnace at temperatures (T_A) in the range of 200-400 °C for 2 h. Thermal stability of the coatings in vacuum (5.0×10^{-4} Pa) was also studied. Accelerated aging tests have been carried out to evaluate the performance of the coatings.

3.0. Results and Discussion

Fig. 1 shows the schematic diagram of the $Cr_xO_y/Cr/Cr_2O_3$ multilayer absorber. The coating consists of a semitransparent Cr metal layer (layer 2 – approx. 13 nm thick) sandwiched between layers of Cr_xO_y and Cr_2O_3. The bottom absorber layer, Cr_xO_y (layer 1- approx. 28 nm thick) has lower oxygen content than the top Cr_2O_3 layer (layer 3 – approx. 64 nm thick). The optimized process parameters are shown in Table 1.

In the $Cr_xO_y/Cr/Cr_2O_3$ coating, the bottom two layers (Cr_xO_y and Cr) act as the main absorber layers and the top Cr_2O_3 layer which has higher oxygen content acts as an antireflection coating. The optimized $Cr_xO_y/Cr/Cr_2O_3$ coating deposited on Cu substrate exhibited a high absorptance of the order of 0.899-0.912 and a low emittance of 0.05-0.06 at 82 °C.

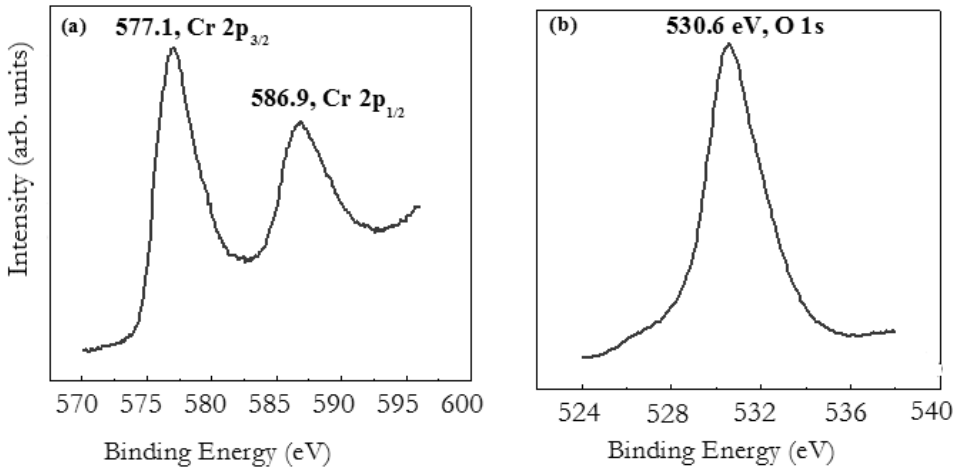

Fig. 2: Core level XPS spectra of: (a) Cr 2p peak and (b) O 1s peak for the as-deposited $Cr_xO_y/Cr/Cr_2O_3$ coating.

Table 2: Effect of 2 h annealing (in air) on the absorptance and emittance values of the $Cr_xO_y/Cr/Cr_2O_3$ coatings deposited on copper substrates.

Annealing Temperature (°C)	α			ε		
	As-deposited	Annealed	$\Delta\alpha$	As-deposited	Annealed	$\Delta\varepsilon$
275	0.899	0.907	+0.008	0.06	0.06	0.00
300	0.898	0.895	-0.003	0.06	0.06	0.00
325	0.909	0.887	-0.012	0.05	0.09	+0.04
350	0.909	0.855	-0.054	0.06	0.24	+0.18

3.1. X-ray photoelectron spectroscopy

Fig. 2 shows high-resolution XPS core level spectra of the as-deposited $Cr_xO_y/Cr/Cr_2O_3$ coating. The spectra were recorded in the near-surface region of the coating. The Cr 2p spectrum (Fig. 2(a)) of the as-deposited $Cr_xO_y/Cr/Cr_2O_3$ coating showed two peaks centered at 577.1 and 586.9 eV, which originate from Cr $2p_{3/2}$ and Cr $2p_{1/2}$, respectively of Cr_2O_3 [14]. The O 1s spectrum (Fig. 2(b)) showed a characteristic peak at a binding energy of 530.6 eV, which corresponds to oxygen in Cr_2O_3 [14]. From the XPS data, it is clear that the near-surface region of the as-deposited $Cr_xO_y/Cr/Cr_2O_3$ coating was rich in chromium oxide. Similar results have been reported in the literature [11]. The XPS data show that the chromium oxide on the near-surface region was in the form of Cr_2O_3 and no phases of CrO_2, CrO_3, etc. were present.

Table 3: Effect of 2 h annealing in vacuum (5.0×10^{-4} Pa) on the absorptance and emittance values of $Cr_xO_y/Cr/Cr_2O_3$ coatings on copper substrates for different temperatures.

Annealing Temperature (°C)	α			ε		
	As-deposited	Annealed	$\Delta\alpha$	As-deposited	Annealed	$\Delta\varepsilon$
400	0.900	0.900	0.000	0.06	0.06	0.00
450	0.901	0.894	-0.007	0.06	0.06	0.00
500	0.899	0.877	-0.022	0.05	0.05	0.00
550	0.910	0.732	-0.178	0.07	0.04	-0.03

3.2. Thermal stability in air

Thermal stability of the solar absorber is very important because the degradation of the absorber at higher operating temperatures causes a decrease in the solar selectivity. The $Cr_xO_y/Cr/Cr_2O_3$ coating deposited on Cu substrate was heat treated in air at different temperatures for 2 h. Values of α and ε for the heat-treated $Cr_xO_y/Cr/Cr_2O_3$ coatings are listed in Table 2. It is clear that the absorptance, emittance and the surface roughness values of the $Cr_xO_y/Cr/Cr_2O_3$ coatings did not change significantly after heat treatment up to 300 °C in air. On the other hand, the emittance and surface roughness values increased drastically for T_A> 300 °C. It has been reported that annealing at temperatures greater than 300 °C results in oxidation of metallic chromium crystallites, which is responsible for optical absorption [15]. This leads to optical degradation in the visible range and decrease of solar absorptance. The increase in the emissivity can be attributed to the diffusion of Cu into the coating and subsequent CuO formation (high ε), which was confirmed by XPS data (data not shown). These data indicate that $Cr_xO_y/Cr/Cr_2O_3$ coating on Cu substrate is thermally stable in air up to 300 °C with a solar selectivity of 0.895/0.06.

The failure of the $Cr_xO_y/Cr/Cr_2O_3$ coating, of the present study, at temperatures above 300 °C is attributed to various factors: i) The fine Cr crystallites in the $Cr_xO_y/Cr/Cr_2O_3$ coating undergo oxidation at T_A> 300 °C and the Cr metal content responsible for the intrinsic optical absorption decreases, resulting in a decrease of the solar absorptance [15]. ii) At T_A> 300 °C, Cu from the substrate started diffusing into the absorber layers. In addition, formation of CuO and the complete intermixing of Cu and Cr ($CuCr_2O_4$) also take place, resulting in an increase in the emittance [16]. At elevated temperatures, the substrate diffusion (i.e., Cu) becomes the dominant degradation effect as a large amount of Cu diffusion leads to a CuO surface layer [15]. iii) For T_A> 300 °C the interdiffusion between Cr and Cr_2O_3 layers is expected to be significant as Cr is reported to be mobile in the Cr_2O_3 layers [16]. iv) Differences in the thermal expansion coefficients of Cr, Cr_2O_3 and Cu substrate, resulting in crack formation and delamination, and subsequent oxidation are also believed to be responsible for the degradation of the coating at higher temperatures.

Table 4: The absorptance and emittance values of the $Cr_xO_y/Cr/Cr_2O_3$ coatings before and after accelerated aging tests.

Temperature (°C)	Time (h)	α			ε		
		As-deposited	Annealed	$\Delta\alpha$	As-deposited	Annealed	$\Delta\varepsilon$
250	250	0.902	0.898	-0.004	0.06	0.11	+0.05
300	25	0.902	0.860	-0.042	0.08	0.15	+0.07
350	15	0.904	0.760	-0.144	0.08	0.26	+0.18

3.3. Thermal stability in vacuum

In order to study the stability of the coatings at higher annealing temperatures, they were heated under high vacuum (5.0×10^{-4} Pa) for 2 h. The absorptance and the emittance values of the $Cr_xO_y/Cr/Cr_2O_3$ coatings after heat-treatment are listed in Table 3. After heat-treatment up to 500 ºC, there was a slight decrease in the absorptance and the emittance remained unchanged. A change in color from blue to brown was observed at $T_A > 500$ ºC along with decreases in absorptance and emittance values. This may be attributed to the diffusion of Cu into the coating [17].

3.4. Accelerated aging tests

Long-term thermal stability of the $Cr_xO_y/Cr/Cr_2O_3$ coatings was studied by conducting accelerated aging tests. The coatings were annealed at temperatures in the range of 250-350 ºC for different durations. Table 4 shows the absorptance and the emittance values of the heat-treated $Cr_xO_y/Cr/Cr_2O_3$ coatings. At $T_A = 250$ ºC (250 h), there was only a minor change in the absorptance and emittance values. But at 350 ºC (15 h) the changes in the absorptance and the emittance were -0.144 and +0.18, respectively.

4.0. Conclusions

- Asymmetric bipolar-pulsed DC generators have been used to deposit $Cr_xO_y/Cr/Cr_2O_3$ solar selective coatings from the reactive sputtering of Cr targets in $Ar+O_2$ and Ar plasmas with high absorptance (0.899-0.912) and low emittance (0.05-0.06).
- Heat-treatment of the $Cr_xO_y/Cr/Cr_2O_3$ coatings in air for 2 h showed that the coatings were stable up to 300 °C with a solar selectivity of 0.895/0.06.
- These coatings were unstable for temperatures greater than 350 °C, because of oxidation of the Cr layer, increased surface roughness (>142 nm) and the formation of CuO.
- The vacuum annealing studies showed marginal change in the absorptance and emittance values up to 500 °C.
- Accelerated aging tests carried out in air for longer durations showed that the coatings were stable up to 250 °C for 250 h with a solar selectivity of 0.898/0.11.

5.0. References

1. Seraphin, B.O.; Solar Energy Conversion: Solid State Physics Aspects: Topics in Applied Physics, edited by Springer, Berlin Vol. 31. 1979.

2. Ritchie, I.T.; Window, B.; Appl. Opt. 1997, vol. 16, p. 1438.
3. Zhang, Q.C.; Mills, D.R.; J. Appl. Phys, 1992, vol. 72, p. 3013.
4. Barshilia, H.C.; Selvakumar, N.; Rajam, K.S.; Rao, D.V.S.; Muraleedharan, K.; Biswas, A.; Appl. Phys. Lett., 2006, vol. 89, p. 191909.
5. Thornton, J.A.; Lamb, J.L.; Thin Solid Films, 1982, vol. 96, p. 175.
6. Schon, J.H.; Binder, G.; Bucher, E.; Sol. Energy Mater. Sol. Cells, 1994, vol. 33, p. 403.
7. Petit, R.N.; Sowell, R.R.; Hall, I.J.; Sol. Energy Mater., 1982, vol. 7, p. 153.
8. Smith, G.B.; Teytz, K.; Hillery, P.; Sol. Energy Mater., 1983, vol. 9, p. 21.
9. Erben,E.; Bertinger, R.; Muhlratzer, A.; Tihanyi, B.; Cornils, B.; Sol. Energy Mater., 1985, vol. 12, p. 239.
10. Fan, J.C.C.; Spura, S.A.; Appl. Phys. Lett., 1977, vol. 30, p. 511.
11. Teixeira, V.; Sousa, E.; Costa, M.F.; Nunes, C.; Rosa, L.; Carvalho, M.J.; Collares-Pereira, M.; Roman, E.; Gago, J.; Vacuum, 2002, vol. 64, p. 299.
12. Gall, D.; Gampp, R.; Lang, H.P.; Oelhafen, P.; J. Vac. Sci. Technol. A, 1996, vol. 14, p. 374.
13. Barshilia, H.C.; Rajam, K.S.; Surf. Coat. Technol., 2006, vol. 201, p. 329.
14. Maetaki, A.; Kishi, K.; Surf. Sci. 1998, vol. 411, p. 35.
15. Zajac, G.; Smith, G.B.; Ignatiev, A.; J. Appl. Phys., 1980, vol. 51, p. 5544.
16. Atkinson, A.; Rev. Mod. Phys., 1985, vol. 57, p. 437.
17. Richharia, P.; Chopra, K.L.; Sol. Energy Mater., 1989, Vol. 19, p. 365.